frontiers | Frontiers in Materials

ORIGINAL RESEARCH
published: 07 July 2022
doi: 10.3389/fmats.2022.956349

Electric-Field Control of Magnetoresistance Behavior in a Conetic Alloy Thin Film/Pb($Mg_{1/3}Nb_{2/3})_{0.7}Ti_{0.3}O_3$ Multiferroic Heterostructure

Cangmin Wang[1], Wenyu Huang[1], Chi Wang[2], Lu Li[2], Chong Wei[2], Yuchen Sun[2], Weifeng Ge[1], Xiaoli Mao[1], Qiang Li[1], Yuanjun Yang[1], Cheng Jia[3], Hui Zhang[3], Zhenlin Luo[4] and Chen Gao[5]**

[1]Department of Physics, Lab of 2D Materials and Quantum Devices, School of Physics, Hefei University of Technology, Hefei, China, [2]School of Microelectronics, Hefei University of Technology, Hefei, China, [3]Department of Physics, University of Science and Technology of China, Hefei, China, [4]National Synchrotron Radiation Laboratory, University of Science and Technology of China, Hefei, China, [5]School of Physical Sciences, University of Chinese Academy of Sciences, Beijing, China

In this work, we investigate the influence of electric fields (E-fields) on the room-temperature magnetotransport behavior of an artificial multiferroic heterostructure, a Conetic alloy ($Ni_{77}Fe_{14}Cu_5Mo_4$) thin film/Pb($Mg_{1/3}Nb_{2/3})_{0.7}Ti_{0.3}O_3$ (011). When the external magnetic field is parallel to the applied current, the switching field increases from 0.8 to 3.3 Oe at 0 and 8 kV/cm, respectively, and the corresponding magnetoresistance (MR) ratio at 20 Oe respectively decreases from 0.14% to 0.03% at 0 and 8 kV/cm. However, when the external magnetic field is perpendicular to the current, the switching field decreases from 10.1 to 1.7 Oe at 0 and 8 kV/cm, and the MR ratio in such a case decreases from –0.001% to –0.10%, respectively. Consequently, under the parallel and perpendicular modes, the tunabilities of the switching field are approximately +313% and –83%, and the MR ratio tunabilities under E-fields are approximately –79% and +9,900%, respectively. Such a large and anisotropic tunability of both the switching field and MR ratio is attributed to the ultrasoft magnetic property of the Conetic alloy thin film and anisotropic in-plane strain-mediated magnetoelectric coupling. However, the anisotropic MR ratio is approximately 0.15% and does not vary with the applied E-fields owing to the intrinsic property of Conetic thin films using transfer and circle transfer curve measurements, rather than the magnetization rotation caused by E-field-induced magnetoelastic anisotropy. This work demonstrates that multiferroic heterostructures with electrically tunable MR show considerable potential in designing energy-efficient electronic and spintronic devices.

Keywords: multiferroic, conetic alloy, ferroelectric, magnetoresistance, magnetoelectric coupling, strain

OPEN ACCESS

Edited by:
Aitian Chen, King Abdullah University of Science and Technology, Saudi Arabia

Reviewed by:
Cai Zhou, Wuhan Textile University, China
Ziyao Zhou, Argonne National Laboratory (DOE), United States

****Correspondence:***
Yuanjun Yang
yangyuanjun@hfut.edu.cn
Chen Gao
gaochen@ucas.ac.cn

Specialty section:
This article was submitted to Quantum Materials, a section of the journal Frontiers in Materials

Received: *30 May 2022*
Accepted: *15 June 2022*
Published: *07 July 2022*

Citation:
Wang C, Huang W, Wang C, Li L, Wei C, Sun Y, Ge W, Mao X, Li Q, Yang Y, Jia C, Zhang H, Luo Z and Gao C (2022) Electric-Field Control of Magnetoresistance Behavior in a Conetic Alloy Thin Film/Pb($Mg_{1/3}Nb_{2/3})_{0.7}Ti_{0.3}O_3$ Multiferroic Heterostructure. Front. Mater. 9:956349. doi: 10.3389/fmats.2022.956349

INTRODUCTION

Writing binary information into magnetic storage devices involves switching the magnetization orientation of magnetic storage units (Brataas et al., 2012). In information storage, electric field (E-field)-controlled magnetism is received widespread attention because it can effectively reduce power consumption during information-writing processes using an E-field strategy (Liu and Sun, 2014; Matsukura et al., 2015; Kumar et al., 2020; Ali et al., 2022). The mechanism by which E-fields regulate magnetism mainly involves five aspects: carrier density (Weisheit et al., 2007), strain (Chen et al., 2019), orbital coupling (Peng et al., 2015), exchange coupling (Wang et al., 2018a), and ion effect (Tan et al., 2019). Among these strategies, strain-driven magnetization switching based on magnetoelectric coupling in composite multiferroic heterostructures is considerably more attractive and has been studied extensively (Motti et al., 2020; Chen et al., 2021; Yang et al., 2021). In such heterostructures, the dynamic strain of the ferroelectric (FE) or piezoelectric component is induced by the converse piezoelectric effect under applied external E-fields and then transferred to the adjacent ferromagnetic layer (Eerenstein et al., 2006). Consequently, the magnetic and electrical properties of composite multiferroic heterostructures, such as coercivity (Tkach et al., 2015), magnetic anisotropy (Wang et al., 2019), magnetization orientation (Wang et al., 2018b), and magnetoresistance (MR), can be controlled using E-fields through the converse magnetostriction effect (Jahjah et al., 2020; Yamada et al., 2021). Recently, Yu et al. (2019) found that the lattice distortion caused by residual compressive strain can induce perpendicular magnetic anisotropy in Co_2MnAl films. Zhou et al. (2021) reported an effective in-plane magnetization 90° rotation induced by the piezo-strain effect in the Co_2FeAl/$Pb(Mg_{1/3}Nb_{2/3})_{0.7}Ti_{0.3}O_3$ (PMN–PT) structure. Yamada et al. (2021) observed that the presence of the magnetoelastic effect owing to spin–orbit interactions at the epitaxial interface between Co_2FeSi and ferroelectric $BaTiO_3$ (001) layers. These studies show great potential for realizing energy-efficient and compact spintronic, and microwave devices using strain-mediated composite multiferroic heterostructures.

In modern spintronics and microelectronics, the MR effects, such as tunneling MR, anisotropic MR (AMR), and giant MR (GMR), have been widely employed in the field of information storage and sensors (Liu and Sun, 2014; Hu and Nan, 2019; Luo et al., 2020). However, in such devices, magnetization orientation and MR modulation are realized under current-induced magnetic fields using a bulky and energy-consumed electromagnet, which will remarkably limit the development of small and ultralow-power spintronic and electronic devices in the future (Hu and Nan, 2019; Wang et al., 2020; Herrera Diez et al., 2021; Ma et al., 2022). Alternatively, by exploiting composite multiferroic heterostructures, the magnetization and subsequent MR can be controlled using E-fields rather than magnetic fields, facilitating the availability of energy-efficient spintronic and electronic devices. Recently, numerous composite multiferroic heterostructures have been proposed and their MR properties have been studied, particularly in Ni-based multiferroic heterostructures. Nan et al. (2015) reported that combined charge and strain-mediated magnetoelectric coupling in an ultrathin NiFe/PMN–PT multiferroic heterostructure, affording the E-field control of reversible and nonvolatile magnetic switching. Gao et al. (2014) studied the voltage-controlled magnetism of the $Ni_{77}Fe_{23}$/PMN–PT (011) multiferroic heterostructure through MR measurement and theoretical analysis. Hong et al. (2016) developed an angle-dependent MR measurement method to study the magnetization rotation in the Ni/SiO_2/Ti/(011)-PMN–PT multiferroic heterostructures. Subsequently, Yang et al. (2017) then used this method to quantify the rotation angle of magnetic anisotropy under the coaction of *in situ* E-fields and magnetic fields in the Ni/(011)-PMN–0.3PT multiferroic heterostructures. Xiong et al. (2018) proved that the $Ni_{81}Fe_{19}$-based multiferroic heterostructure can also achieve a large magnetoelectric coupling at room temperature, yielding a tunability of magnetic anisotropy up to 332 fJ/Vm. Du et al. (2020) observed a large, nonvolatile, and tunable magnetization switching in the $Ni_{80}Co_{20}$ alloy film/PMN–PT multiferroic heterostructure at room temperature. These great achievements in Ni-based magnetic films/ferroelectrics multiferroic heterostructures would enable a promising application in novel spintronic devices.

Motivated by aforementioned achievements in the Ni-based magnetic alloys for multiferroic heterostructures, we explored a well-known mu-metal series of ultrasoft magnetic material (a typical representative Conetic alloy: $Ni_{77}Fe_{14}Cu_5Mo_4$) as a ferromagnetic component to create Conetic alloy thin film/PMN–PT multiferroic heterostructures. The $Ni_{77}Fe_{14}Cu_5Mo_4$ alloy exhibit relatively smaller easy-axis (e.a.) coercivity, larger hard-axis magnetic susceptibility and higher attenuation (Choi et al., 2010; Lei et al., 2011). Consequently, they are widely used in many spintronic devices as sensing or composite free layers in AMR sensors for hysteresis-free and linear field responses and magnetic tunnel junctions for large TMR ratio (Egelhoff et al., 2010). Therefore, aiming to develop novel spintronic materials for technical applications, we fabricated Conetic alloy thin films using magnetron sputter technique and studied E-field control of MR and magnetization switching behavior using transfer curve (TC) and circle transfer curve (CTC) measurements in the $Ni_{77}Fe_{14}Cu_5Mo_4$/(011)-PMN–PT multiferroic heterostructure. We found that switching fields and the MR ratio were anisotropically controlled by E-fields with a giant tunability. Such a Conetic alloy thin film/PMN–PT multiferroic heterostructure demonstrates strong magnetoelectric coupling, regardless of the weak magnetostriction in the Conetic alloy thin film, showing its potential in ultralow-power spintronic devices.

EXPERIMENTAL DETAILS

We deposited Conetic alloy ($Ni_{77}Fe_{14}Cu_5Mo_4$) thin films on the (011)-cut PMN–PT substrates using a custom multi-target high-vacuum magnetron sputtering system (base pressure better than 4.5×10^{-8} Torr) (Egelhoff et al., 2010). The sputter power was set to 15 W. The growth environment comprised a constant Ar pressure of 2.3 mTorr. The film thickness was calibrated to be

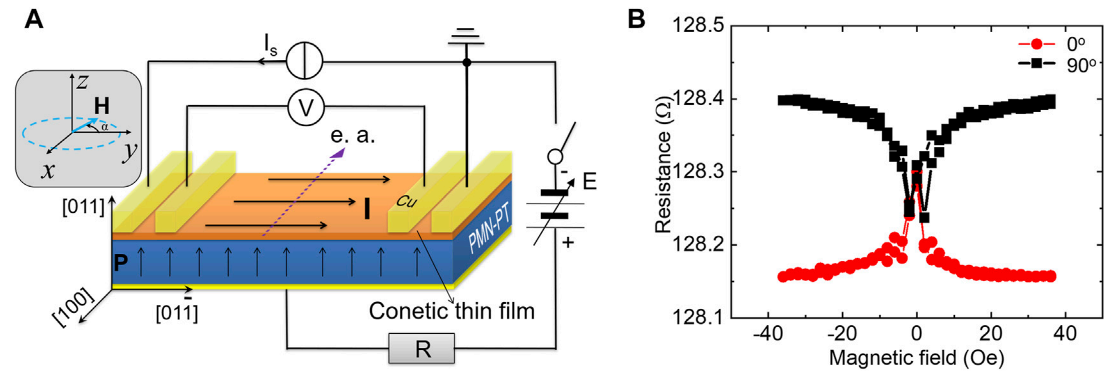

FIGURE 1 | (A) Schematic of a Conetic alloy thin film/PMN–PT multiferroic heterostructure. The four-probe MR measurement and *in situ* E-field application are also shown here. **(B)** MR as a function of the applied in-plane magnetic field H toward $\alpha = 0^{\circ}$ and 90°. Herein, α is the angle between the in-plane magnetic field and y-axis (or current I), as illustrated in the upper left corner of Figure 1. Magnetic field H scans back and forth between −36 and +36 Oe. Herein, the ferroelectric substrate PMN-PT was in a unpolarized state.

10 nm by carefully controlling the deposition time. During the sputtering process, the substrates were rotated at a constant speed to ensure uniformity throughout the sample. Then the Cu pads were deposited *ex situ* at room temperature using the e-beam method by employing a four-probe shadow mask. For magnetoresistance measurements, the magnetic field scanning rate was 2 s per step for one recording data, while E-fields were still maintained along the thickness direction of the PMN–PT. The minimum resistance of the PMN–PT substrate was 2 G·Ω during the scanning of E-fields so that the leakage current could be ignored during magnetotransport measurements. (Zhang et al., 2011).

RESULTS AND DISCUSSION

Device Architecture and Magnetotransport Properties

Figure 1A presents a schematic of the Conetic alloy thin-film/PMN–PT multiferroic heterostructure device used for the measurement. The e.a. was set along the [100] direction of the PMN–PT substrate using magnetic thermal annealing treatment (Yang et al., 2021). MR was measured using a four-probe technique with current I (black solid line) along the [01 $\bar{1}$] direction of the PMN–PT substrate. E-fields were applied along the thickness direction of the substrate. External magnetic fields were sequentially applied along the multiferroic heterostructure plane and could be rotated at a constant magnitude (α is the angle of rotation of the magnetic field), as shown in the upper left corner of **Figure 1**. The MR curves of the Conetic alloy thin film at $\alpha = 0^{o}$ and 90^{o} on the unpolarized PMN-PT ferroelectric layer are a function of the applied magnetic fields as shown in **Figure 1B**. Overall, when scanning the magnetic field in the forward and reverse directions, both MR curves show weak hysteresis characteristics, indicating excellent soft magnetic properties of the Conetic alloy thin film. In the MR measurement, when the magnetic field is rotated at 90° (dotted line), magnetization is almost completely along the e.a., resulting in a small change in the resistance of the Conetic alloy thin film. Herein, the magnetization perpendicular to *I* is termed the perpendicular mode and that parallel to *I* is called the parallel mode. Because magnetization was perpendicular to *I*, MR is smaller than that obtained at 0° (square line) under the concerned magnetic fields, where magnetization was parallel to *I*. Consequently, a large change is observed in the resistance owing to the AMR effect. This result is consistent with previous reports on permalloy thin films (García et al., 2006; Krzyk et al., 2010). Based on these two curves, the AMR ratio can be extracted using the following formula (Rüffer et al., 2014):

$$\text{AMR ratio} = \frac{R_{\parallel} - R_{\perp}}{R_{\perp}} \times 100\% \quad (1)$$

where $R_{\parallel}$ and $R_{\perp}$ are the maximal and minimal MR values when the magnetic fields are parallel and perpendicular to ***I***, respectively (Aharoni et al., 2000). Therefore, the AMR ratio measured at the initial state (i.e., unpolarized state) is ~0.15%, comparable to the value of ~0.85% for a 10-nm-thick $Ni_{80}Fe_{20}$ thin film on a (100) p-Si substrate (Kateb and Ingvarsson, 2017) and ~0.48% for a 20-nm-thick $Ni_{81}Fe_{19}$/glass thin film (Wang et al., 2013). The relatively slight decrease in the AMR ratio in the $Ni_{77}Fe_{14}Cu_{5}Mo_{4}$ thin films is considerably attributed to the vacuum pressure, temperature and time in the annealing treatment (Zhao et al., 2013), which will be investigated in the future.

E-Field Control of Switching Field

To study the influence of E-fields on the magnetotransport characteristics of the Conetic alloy thin film/PMN–PT multiferroic heterostructures, MR was measured along the anisotropic [100] and [01 $\bar{1}$] directions of the PMN-PT substrate under different unipolar E-fields while performing transfer curve measurements. In the parallel mode (inset of **Figure 2A**), the parallel resistance increases sharply with an increase in the magnetic field and reaches saturation at ~20 Oe, indicating a normal MR effect in the Conetic thin film (Guo et al., 2018). Furthermore, the typical hard-axis

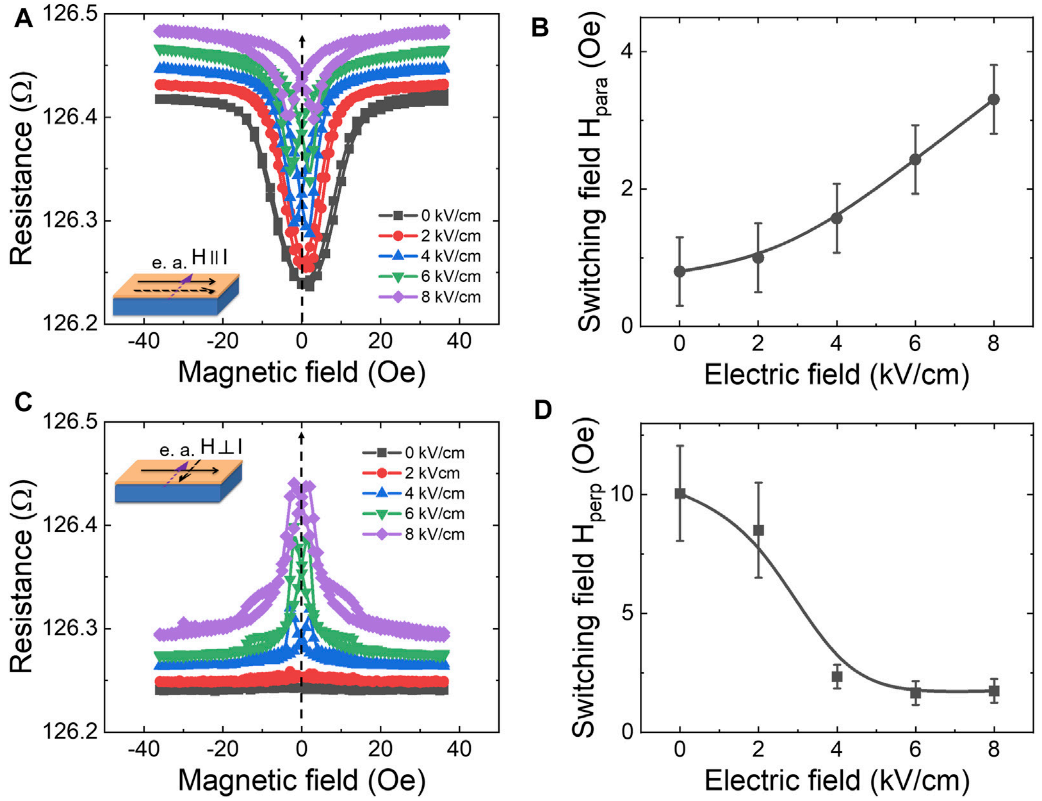

FIGURE 2 | (A) and **(C)** Magnetoresistance in the Conetic alloy thin film/PMN–PT multiferroic heterostructure as a function of the applied magnetic field with different bias E-fields. Magnetic field H (black dotted line) is parallel and perpendicular to current I (black solid line) in the inset of Panels **(A,C)**, respectively. **(B)** and **(D)** Dependence of the switching field on the E-fields in the Conetic alloy thin film/PMN–PT multiferroic heterostructure when the magnetic fields are along [01 $\bar{1}$] and [100] directions of the FE layer, respectively.

resistance curve shows only a small hysteresis under zero magnetic fields in the absence of E-fields. Under applied E-fields, double-peak resistance curves are detected. These peaks are attributed to the reversal of magnetization in the magnetic domains owing to the reversal of the magnetic fields, corresponding to the switching field in the multiferroic heterostructure (Zhou et al., 2017). **Figure 2B** presents the variation in the switching field H_{para} (the subscript is shorten of the parallel mode) with the E-field. In this parallel mode, the switching field increases substantially and linearly with the E-field from ~0.8 to 3.3 Oe at 0 and 8 kV/cm, respectively. Correspondingly, the tunability of the switching field is +313% under the magnetic field along the [01 $\bar{1}$] direction in the parallel mode. The tunability is calculated using the following formula:

$$\left[H_{para}(8KV/cm) - H_{para}(0KV/cm)\right] / H_{para}(0KV/cm) \times 100\% \quad (2)$$

where H_{para} (8 kV/cm) and H_{para} (0 kV/cm) are the switching fields at 8 and 0 kV/cm, respectively. In the perpendicular mode (inset of **Figure 2C**), the MR decreases, showing a negative MR effect with increasing magnetic fields. This result is attributed to the AMR effect (Hong et al., 2016). When increasing the E-field, the amount of resistance change increases, yielding an obvious bimodal hysteresis curve (**Figure 2C**). Accordingly, the switching field H_{perp} (the subscript refers to the perpendicular mode) as a function of the E-field is shown in **Figure 2D**. The switching field decreases from ~10.1 to 1.7 Oe at 0 and 8 kV/cm, respectively. Consequently, the tunability of the switching field induced by E-fields is up to −83% in the perpendicular mode. These results show that the E-field can considerably modulate the switching field of the Conetic alloy thin film/PMN–PT multiferroic heterostructure. In particular, the switching field shows anisotropic tunability when the magnetic field is along the [100] and [01 $\bar{1}$] directions of the PMN–PT FE layer, implying that strain-mediated magnetoelectric coupling should be the dominant mechanism in the E-field control of the switching field in our heterostructure (Motti et al., 2020; Chen et al., 2021; Yang et al., 2021). The corresponding anisotropic strain along the [100] and [01 $\bar{1}$] directions is also shown in order to further verify this anisotropic magnetoelectric coupling (see details in **Supplementary Figure S1** in the Supplementary Material).

E-Field Control of Magnetoresistance

We also extract the MR dependence on E-fields using **Figures 2A,C**. As shown in **Figures 3A,B**, the parallel MR ratio (i.e., in the parallel mode) is defined as (Zhou et al., 2017)

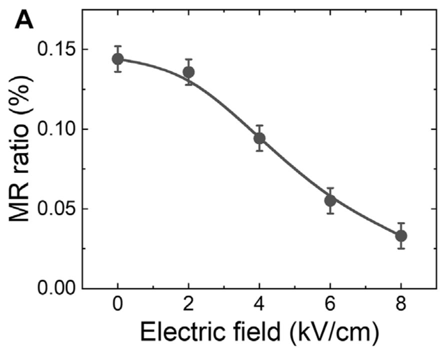

FIGURE 3 | (A) and **(B)** Magnetoresistance ratio under parallel and perpendicular modes, respectively. Herein, magnitude of the magnetic field is set to ~20 Oe to illustrate the E-field modulation of spin-dependent transport behavior.

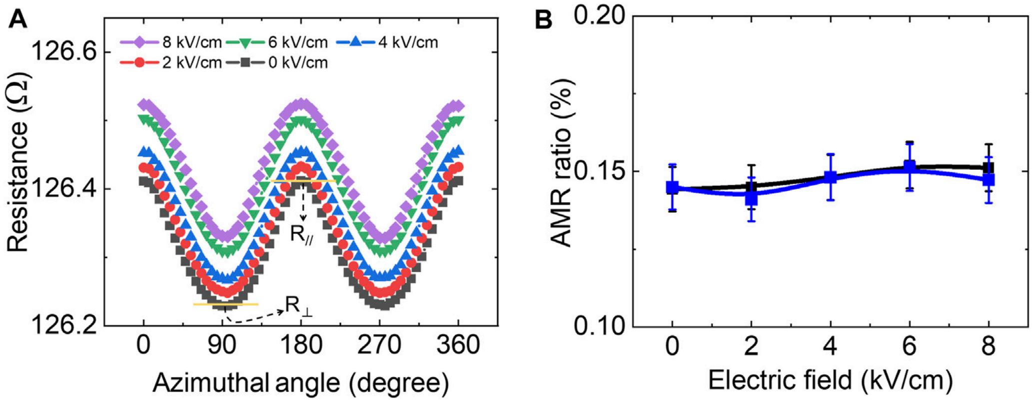

FIGURE 4 | (A) Circle transfer curves under different E-field bias. The saturated magnetic field ~35 Oe was chosen to perform this measurement. $R_{\perp}$ and $R_{\parallel}$ is minimal and maximal magnetoresistance value in the CTCs, respectively. **(B)** AMR ratio is as a function of the applied electric fields. The black and blue symbols represent the AMR ratio derived by TC and CTC measurements, respectively.

$$\text{MR ratio} = \Delta R/R = [R(H) - R(0)]/R(0) \times 100\% \quad (3)$$

where $R(H)$ and $R(0)$ are the resistance of the Conetic alloy thin film in magnetic field **H** and a zero magnetic field, respectively. Herein, $R(H)$ value is extract from the major and minor TCs as magnetic field H is 20 Oe. The parallel MR ratio in such a configuration decreases from ~0.14% to 0.03% at 0 and 8 kV/cm, respectively (**Figure 3A**). This decrease in the MR ratio is ascribed to an increase in the resistivity and a decrease in the magnitude of the resistance change caused by E-field modulations (Liu et al., 2011). Hence, as the magnetic field is along the [01 $\bar{1}$] direction of the FE layer, the tunability of the MR ratio induced by the electric field is ~−79% as mentioned in **Eq. 2**, which is also calculated according to the tunability of the switching field. Unlike in the case of the parallel mode, the MR ratio under the perpendicular mode decreases from approximately −0.001% to −0.10% at 0 and 8 kV/cm, respectively, which is attributed to a large change in the resistance, even though the resistance itself increases owing to the E-fields. Consequently, the tunability of the perpendicular MR ratio of up to approximately +9,900% is achieved when the magnetic field is oriented along the [100] direction of the FE layer. These results indicate the large and anisotropic tunability of the MR ratio, possibly ascribed to the magnetization orientation of the Conetic alloy thin film induced by anisotropic in-plane strain-mediated magnetoelectric coupling. It is mentionable that the E-field control of switching fields and MR ratio are volatile due to unipolar E-field cycling scheme here. Non-volatile E-field control of them can be expected using bipolar E-field cycling means as reported previously (Hu and Nan, 2019; Chen et al., 2021).

As mentioned above, MR ratio under weak magnetic field bias can be remarkably modulated by E-fields. Now we turn to examine the AMR ratio controlled by E-fields under large and even saturated magnetic field bias. **Figure 4A** shows circle transfer curves (CTCs) under a saturated magnetic field (H = 35 Oe). According to $R_{\perp}$ and $R_{\parallel}$ value as labelled in **Figure 4A**, we can calculate the AMR ratio using **formula (1)**. The corresponding AMR ratio is summarized in **Figure 4B** as shown by black line. Additionally, we also check the AMR ratio marked by blue line in **Figure 4B** using the MR data,

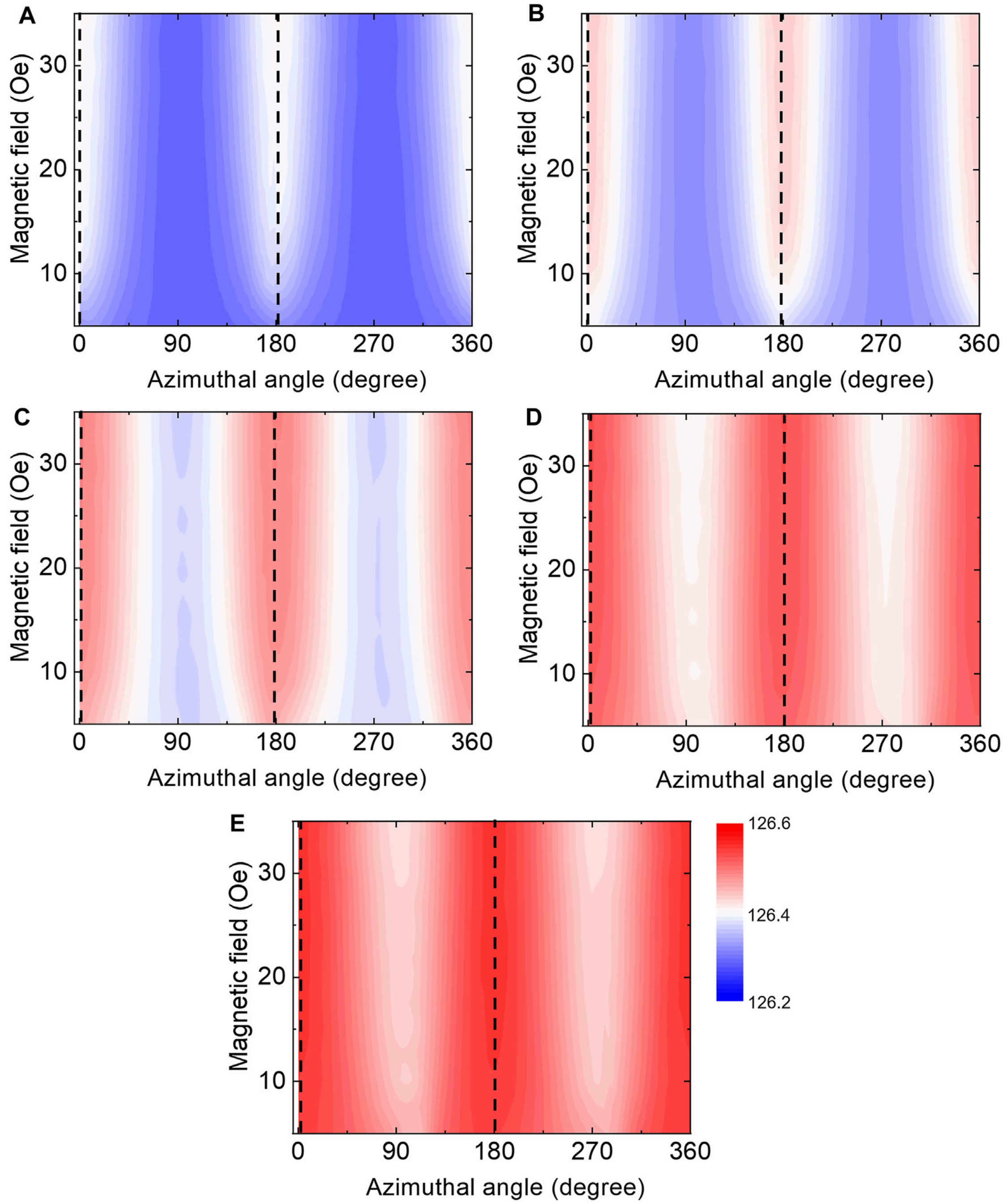

FIGURE 5 | (A–E) CTC mappings under different E-field bias, i.e., 0, 2, 4, 6, and 8 kV/cm, respectively. The dashed lines show the angular position of applied magnetic fields with maximum magnetoresistance values. All figures use same contour scale with unit Ω.

which is extracted from TC measurements at 0, 2, 4, 6, and 8 kV/cm as previously shown in **Figures 2A,C**. On the one hand, these two methods are in good agreement. On the other hand, the AMR ratio barely changes within the tolerance range as the E-field increases. The corresponding average value of the AMR ratio is approximately 0.15%. Currently, the widely accepted physical mechanism is that the AMR effect is an intrinsic material property owing to the anisotropic scattering of the conducted electrons and local *d* electrons in magnetic alloy (Potter, 1974; Chattopadhyay et al., 2002). Therefore, the strain-mediated magnetoelectric coupling in our multiferroic heterostructure can modulate the switching field and MR behavior at relatively small magnetic field bias, rather than tune the AMR ratio at large and even saturated magnetic field bias, which is also observed in Co/PMN–PT (011) and $Ni_{80}Co_{20}$/PZN-PT (011) multiferroic

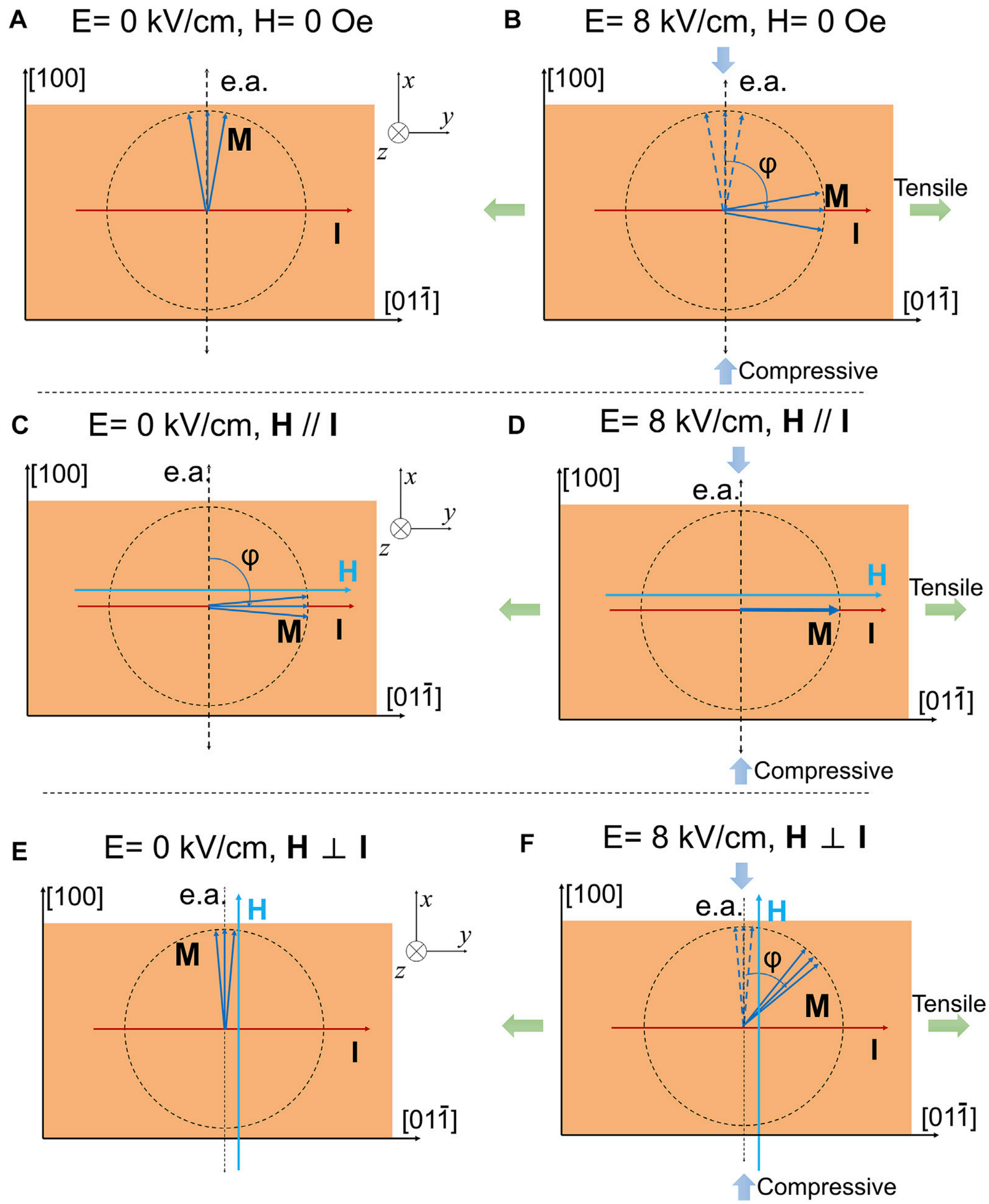

FIGURE 6 | (A) Schematic of the initial magnetic state of the Conetic alloy thin film/PMN–PT multiferroic heterostructure. **(B)** Schematic of magnetization rotation induced by E-field-induced tensile and compressive strains without magnetic field bias. Wide, light blue and green arrows represent in-plane anisotropic compressive and tensile strains, respectively. **(C)** and **(D)** Schematics of magnetic states at 0 and 8 kV/cm, respectively, with the magnetic field perpendicular to current **(I)**. **(E)** and **(F)** Schematics of magnetic states at 0 and 8 kV/cm, respectively, with the magnetic field parallel to current **(I)**. Light blue, dark blue and dark red arrows represent magnetic field H, magnetization M and applied current I, respectively. The thick, dark blue arrow in Panel **(D)** means that the magnetization is almost aligned along the [01 $\bar{1}$] direction of the PMN-PT under application of E-fields.

heterostructures (Liu et al., 2011; Zhou et al., 2017). It is mentionable that the ferroelectric polarization induced interfacial charge has no effects on the E-field control of switching fields and MR behaviors due to the short charge-screening length of the metallic ferromagnet Conetic films studied here (Hu and Nan, 2019).

Mechanism of E-Field Control of Switching Field and Magnetoresistance

In order to reveal mechanism of E-field control of switching fields and magnetoresistance behavior (Yang et al., 2021), CTC mappings are performed by scanning magnetic fields from 5 to 35 Oe in a step 5 Oe under E-fields of 0, 2, 4, 6, and 8 kV/cm as shown in **Figures 5A–E**, respectively. First, considering any of the data plots in **Figure 5**, the azimuthal position of the maximal value of the MR does not change as marked by dashed lines, either at 0° or at 180°. It is almost the same as the magnetic field rotation direction, strongly indicating ultrasoft magnetic properties of the Conetic thin films (Lei et al., 2011). Second, comparing the CTC mapping results under different E-fields, the applied electric field makes the contour darker, that is, the MR becomes larger, which is also consistent with the TC measurements. Additionally, the position of the maximal magnetoresistance does not move when the electric field is applied, implying that the direction of E-field-induced magnetoelastic anisotropy is exactly along the [01 $\bar{1}$] direction, so that the magnetization favors to stay in this direction (Nan et al., 2015; Zhou et al., 2021).

According to the above experimental results, we further phenomenologically analyze magnetization rotation through energy competitions among the Zeeman, uniaxial magnetic anisotropic, and magnetoelastic anisotropic energies induced by E-fields in a single-domain mode. As shown in **Figures 6A,B**, when an E-field is applied to the FE layer, an anisotropic in-plane strain is generated [compressive strain ($\sigma_x < 0$) along the [100] direction and tensile strain ($\sigma_y > 0$) along the [01 $\bar{1}$] direction] by the converse piezoelectric effect (Zhang et al., 2015). Hence the in-plane magnetoelastic anisotropic energy can be expressed using following formula (Liu et al., 2010):

$$F_{\mathrm{me}} = -\frac{3}{2}\lambda_s\sigma_x\cos^2\varphi - \frac{3}{2}\lambda_s\sigma_y\sin^2\varphi \quad (4)$$

where φ represents the angle between the magnetization and strain direction of σ_x (**Figure 6**). λ_s (>0) represents the saturated magnetostriction coefficient of the Conetic alloy thin film (Klokholm and Aboaf, 1981; Egelhoff et al., 2006). To accommodate the E-field-induced magnetoelastic anisotropy energy, the magnetization seeks the lowest energy orientation on the free energy surface (Liu et al., 2010). Qualitatively, the lowest magnetoelastic energy can be obtained as a product of magnetoelastic energy terms $\lambda_s\sigma_x$ and $\lambda_s\sigma_y$. Assuming that the in-plane anisotropic strain in the PMN–PT layer can be completely transferred to the Conetic alloy thin film, the magnetoelastic energy terms $\lambda_s\sigma_x$ and $\lambda_s\sigma_y$ under a nonzero unipolar E-field are negative and positive along the [100] and [01 $\bar{1}$] directions of the FE layer, respectively. Thus, the E-field-induced magnetoelastic anisotropy energy induces the rotation of the magnetic e.a. from the [100] to the [01 $\bar{1}$] direction of the FE layer. Subsequently, the magnetization will rotate from the [100] direction (i.e., e.a. direction; **Figure 6A**) to the [01 $\bar{1}$] direction of the FE layer as shown in **Figure 6B**, increasing the MR because of the AMR effect (Wang et al., 2019; Yamada et al., 2021; Zhou et al., 2021). Therefore, regardless of whether the magnetic field is along the [100] or [01 $\bar{1}$] direction, MR increases after applying the E-fields, which is also illustrated by the dashed arrows in **Figures 2A,B**.

Furthermore, in the parallel mode, the applied magnetic field will rotate the magnetization and distribute spatially it along the [01 $\bar{1}$] direction of the FE layer owing to the soft magnetic property of the Conetic alloy thin film in the absence of the E-field as shown in **Figure 6C**. After applying the E-fields, the magnetization is strictly oriented along the [01 $\bar{1}$] direction (**Figure 6D**) because of the addition of the E-field-induced magnetoelastic anisotropy (Wang et al., 2018a; Wang et al., 2019; Du et al., 2020). Consequently, the switching field increases, as evidenced (**Figure 2B**), and the MR increases; however, its change reduces, thereby decreasing the MR ratio (**Figure 3A**). However, in the perpendicular mode, the applied magnetic field attempts to align the magnetization along the [100] direction (i.e., e.a.) of the FE layer as shown in **Figure 6E**. When applying the E-fields, the magnetization rotates toward the [01 $\bar{1}$] direction as shown in **Figure 6F** owing to the aforementioned strain-mediated magnetoelectric coupling. Therefore, the magnetization along the [100] direction of the FE layer is easier to reverse with the assistance of the E-field-induced magnetoelastic anisotropy than that in the absence of E-fields (Yang et al., 2021; Zhou et al., 2021), thus decreasing the switching field (**Figure 2D**). Moreover, the MR decreases considerably, thereby increasing the MR ratio (**Figure 3B**). Based on these analyses, the giant and anisotropic tunability of the switching field and MR ratio is mainly attributed to the in-plane anisotropic strain-mediated magnetoelectric coupling between the Conetic alloy thin film and (011)-PMN–PT FE layer and ultrasoft magnetic property of the Conetic film, in addition to ultrasoft magnetic property of the Conetic thin film. However, the in-plane strain induced by ferroelastic domain switching should be neglected due to the unipolar E-field cycling here rather than bipolar cycling in previous report (Zhang et al., 2012).

CONCLUSION

In conclusion, to develop novel spintronic materials for technical applications, we fabricated a Conetic alloy thin film/PMN–PT multiferroic heterostructure. We observed that the magnetotransport properties are considerably modulated by the E-fields. The tunabilities of the switching field are approximately +313% and −83% under the parallel and perpendicular modes, respectively. Furthermore, the tunability of the MR ratio induced by the E-field is respectively up to approximately −79% and +9,900% under the parallel and perpendicular modes. These results indicate a large and anisotropic tunability of both the switching field and MR ratio because of the change in the magnetization orientation induced by anisotropic in-plane strain-mediated magnetoelectric coupling and ultrasoft magnetic property of the Conetic alloy thin film. However, the AMR ratio is almost unaffected by the E-fields because the AMR effect is an intrinsic property of the Conetic alloy thin film. This work deepens the understanding of the electrical manipulation of magnetic anisotropy in the multiferroic heterostructure. Furthermore, the E-field control of the switching field and MR offers a promising opportunity for further optimizing the Conetic alloy-based spintronic devices in the future.

DATA AVAILABILITY STATEMENT

The original contributions presented in the study are included in the article/**Supplementary Material**, further inquiries can be directed to the corresponding authors.

AUTHOR CONTRIBUTIONS

YY and CG conceptualized this work. CaW, WH, ChW, and WG fabricated the samples. CaW, LL, CoW, and YS performed magnetoresistance measurements and collected experimental data. XM, QL, CJ, HZ, and ZL conducted data analysis and discussed with other authors. YY, HZ, and CG looked for funding acquisition for this work. CaW wrote the paper, and all authors revised it.

FUNDING

This work was mainly funded from the National Natural Science Foundation of China (52072102, 11775224, 12074357, and 11804324), partially supported by the Open Foundation of the University of Science and Technology of China (KF2020002), National Key Research and Development Program of China (2017YFA0205004) and Chinese Academy of Sciences Pioneer Hundred Talents Program.

ACKNOWLEDGMENTS

We also gratefully acknowledge the beamlines BL07W, BL11U, and BL12B-α at the National Synchrotron Radiation Laboratory (NSRL) for the device fabrications and property characterizations.

SUPPLEMENTARY MATERIAL

The Supplementary Material for this article can be found online at: https://www.frontiersin.org/articles/10.3389/fmats.2022.956349/full#supplementary-material

REFERENCES

Aharoni, A., Pust, L., and Kief, M. (2000). Comparing Theoretical Demagnetizing Factors with the Observed Saturation Process in Rectangular Shields. *J. Appl. Phys.* 87, 6564–6566. doi:10.1063/1.372771

Ali, I., Hussan, G., and Ahmed, S. (2022). Fabrication of Self-Healing Hybrid Nanogenerators Based on Polyurethane and ZnO for Harvesting Wind Energy. *J. Mat. Sci. Mat. Electron* 33, 8048. doi:10.1007/s10854-021-07591-x

Brataas, A., Kent, A. D., and Ohno, H. (2012). Current-induced Torques in Magnetic Materials. *Nat. Mater* 11, 372–381. doi:10.1038/nmat3311

Chattopadhyay, M. K., Roy, S. B., Chaudhary, S., Jeet Singh, K., and Nigam, A. K. (2002). Magnetic Response ofFe1−xCoxSialloys: A Detailed Study of Magnetization and Magnetoresistance. *Phys. Rev. B* 66, 174421. doi:10.1103/physrevb.66.174421

Chen, A., Piao, H., Ji, M., Fang, B., Wen, Y., Ma, Y., et al. (2021). Using Dipole Interaction to Achieve Nonvolatile Voltage Control of Magnetism in Multiferroic Heterostructures. *Adv. Mat.* 23, 2105902. doi:10.1002/adma.202105902

Chen, X., Zhou, X., Cheng, R., Song, C., Zhang, J., Wu, Y., et al. (2019). Electric Field Control of Néel Spin-Orbit Torque in an Antiferromagnet. *Nat. Mat.* 18, 931–935. doi:10.1038/s41563-019-0424-2

Choi, J.-G., Hwang, D.-G., Rhee, J.-R., and Lee, S.-S. (2010). Comparison of the Soft Magnetic Properties of Permalloy and Conetic Thin Films. *J. Magnetism Magnetic Mater.* 322, 2191–2194. doi:10.1016/j.jmmm.2010.02.008

Du, W., Liu, M., Su, H., Zhang, H., Liu, B., Meng, H., et al. (2020). Wide Range Voltage-Impulse-Controlled Nonvolatile Magnetic Memory in Magnetoelectric Heterostructure. *Appl. Phys. Lett.* 117, 222401. doi:10.1063/5.0033319

Eerenstein, W., Mathur, N. D., and Scott, J. F. (2006). Multiferroic and Magnetoelectric Materials. *Nature* 442, 759–765. doi:10.1038/nature05023

Egelhoff, W. F., Jr., Höink, V. E., Lau, J. W., Shen, W. F., Schrag, B. D., and Xiao, G. (2010). Magnetic Tunnel Junctions with Large Tunneling Magnetoresistance and Small Saturation Fields. *J. Appl. Phys.* 107, 09C705. doi:10.1063/1.3358609

Egelhoff, W. F., McMichael, R. D., Dennis, C. L., Stiles, M. D., Johnson, F., Shapiro, A. J., et al. (2006). Soft Magnetic Layers for Low-Field-Detection Magnetic Sensors. *Thin Solid Films* 505, 90–92. doi:10.1016/j.tsf.2005.10.014

Gao, Y., Hu, J., Shu, L., and Nan, C. W. (2014). Strain-mediated Voltage Control of Magnetism in Multiferroic Ni77Fe23/Pb(Mg1/3Nb2/3)0.7Ti0.3O3 Heterostructure. *Appl. Phys. Lett.* 104, 142908. doi:10.1063/1.4870975

García, N., Hao, C., Yonghua, L., Muñoz, M., Chen, Y., Cui, Z., et al. (2006). Is There Ballistic Transport in Metallic Nano-Objects? Ballistic versus Diffusive Contributions. *Appl. Phys. Lett.* 89, 083112. doi:10.1088/0953-8984/19/1/016212

Guo, Q., Xu, X., Wang, F., Lu, Y., Chen, J., Wu, Y., et al. (2018). In-plane Electric Field Controlled Ferromagnetism and Anisotropic Magnetoresistance in an LSMO/PMN-PT Heterostructure. *Nanotechnology* 29, 224003. doi:10.1088/1361-6528/aab5fb

Herrera Diez, L., Kruk, R., Leistner, K., and Sort, J. (2021). Magnetoelectric Materials, Phenomena, and Devices. *Apl. Mater.* 9, 050401. doi:10.1063/5.0053631

Hong, B., Yang, Y., Zhao, J., Hu, K., Peng, J., Zhang, H., et al. (2016). Quantifying Electric-Field Control of Magnetization Rotation in Ni/SiO2/Ti/(011)-PMN-PT Multiferroic Heterostructures via Anisotropic Magnetoresistance Measurements. *Mater. Lett.* 169, 110–113. doi:10.1016/j.matlet.2016.01.109

Hu, J.-M., and Nan, C.-W. (2019). Opportunities and Challenges for Magnetoelectric Devices. *Apl. Mater.* 7, 080905. doi:10.1063/1.5112089

Jahjah, W., Jay, J.-Ph., Le Grand, Y., Fessant, A., Prinsloo, A. R. E., Sheppard, C. J., et al. (2020). Electrical Manipulation of Magnetic Anisotropy in a Fe81Ga19/Pb (Mg1/3Nb2/3)O3-Pb (ZrxTi1 -x)O3 Magnetoelectric Multiferroic Composite. *Phys. Rev. Appl.* 13, 034015. doi:10.1103/PhysRevApplied.13.034015

Kateb, M., and Ingvarsson, S. (2017). “SAS 2017 - 2017 IEEE Sensors Applications Symposium,” in 2017 IEEE Sensors Applications Symposium (SAS), 2017.3.13-2017.3.15 (Glassboro, NJ, USA: IEEE), 1–5. doi:10.1109/SAS.2017.7894043

Klokholm, E., and Aboaf, J. A. (1981). The Saturation Magnetostriction of Permalloy Films. *J. Appl. Phys.* 52, 2474–2476. doi:10.1063/1.328971

Krzyk, S., Schmidsfeld, A., Kläui, M., and Rüdiger, U. (2010). Magnetotransport Effects of Ultrathin Ni80Fe20films Probedin Situ. *New J. Phys.* 12, 013001. doi:10.1088/1367-2630/12/1/013001

Kumar, M., Shankar, S., Kumar, A., Anshul, A., Jayasimhadri, M., and Thakur, O. P. (2020). Progress in Multiferroic and Magnetoelectric Materials: Applications, Opportunities and Challenges. *J. Mat. Sci. Mat. Electron* 31, 19487–19510. doi:10.1007/s10854-020-04574-2

Lei, Z. Q., Li, G. J., Egelhoff, W. F., Lai, P. T., and Pong, P. W. T. (2011). Magnetic Tunnel Junction Sensors with Conetic Alloy. *IEEE Trans. Magn.* 47, 714–717. doi:10.1109/tmag.2010.2104136

Liu, M., Li, S., Obi, O., Lou, J., Rand, S., and Sun, N. X. (2011). Electric Field Modulation of Magnetoresistance in Multiferroic Heterostructures for Ultralow Power Electronics. *Appl. Phys. Lett.* 98, 222509. doi:10.1063/1.3597796

Liu, M., Obi, O., Cai, Z., Lou, J., Yang, G., Ziemer, K. S., et al. (2010). Electrical Tuning of Magnetism in Fe3O4/PZN-PT Multiferroic Heterostructures Derived by Reactive Magnetron Sputtering. *J. Appl. Phys.* 107, 073916. doi:10.1063/1.3354104

Liu, M., and Sun, N. X. (2014). Voltage Control of Magnetism in Multiferroic Heterostructures. *Phil. Trans. R. Soc. A* 372, 20120439. doi:10.1098/rsta.2012.0439

Luo, J., Zhang, Y., Ou-Yang, J., and Yang, X. (2020). Electric Field-Controlled Anisotropic Magnetoresistance Effect with Four-Fold-Symmetric Magnetic Anisotropy. *Ceram. Int.* 46, 13732–13736. doi:10.1016/j.ceramint.2020.02.161

Ma, M., Tao, Z., Ren, X., Cao, H., Yin, X., Han, Y., et al. (2022). Electric Field Manipulation of Transport Properties for Ultra-thin Fe70Ga30 Films on

BaZr0.2Ti0.8O3-0.5Ba0.7Ca0.3TiO3 Films. *J. Mat. Sci. Mat. Electron* 33, 7995–8002. doi:10.1007/s10854-022-07950-2

Matsukura, F., Tokura, Y., and Ohno, H. (2015). Control of Magnetism by Electric Fields. *Nat. Nanotech* 10, 209–220. doi:10.1038/nnano.2015.22

Motti, F., Vinai, G., Bonanni, V., Polewczyk, V., Mantegazza, P., Forrest, T., et al. (2020). Interplay between Morphology and Magnetoelectric Coupling in Fe/PMN-PT Multiferroic Heterostructures Studied by Microscopy Techniques. *Phys. Rev. Mater.* 4, 114418. doi:10.1103/physrevmaterials.4.114418

Nan, T., Zhou, Z., Liu, M., Yang, X., Gao, Y., Assaf, B. A., et al. (2015). Quantification of Strain and Charge Co-mediated Magnetoelectric Coupling on Ultra-thin Permalloy/PMN-PT Interface. *Sci. Rep.* 4, 3688. doi:10.1038/srep03688

Peng, J., Song, C., Li, F., Cui, B., Mao, H., Wang, Y., et al. (2015). Charge Transfer and Orbital Reconstruction in Strain-Engineered (La,Sr)MnO3/LaNiO3 Heterostructures. *ACS Appl. Mat. Interfaces* 7, 17700–17706. doi:10.1021/acsami.5b04994

Potter, R. I. (1974). Magnetoresistance Anisotropy in Ferromagnetic NiCu Alloys. *Phys. Rev. B* 10, 4626–4636. doi:10.1103/physrevb.10.4626

Rüffer, D., Slot, M., Huber, R., Schwarze, T., Heimbach, F., Tütüncüoglu, G., et al. (2014). Anisotropic Magnetoresistance of Individual CoFeB and Ni Nanotubes with Values of up to 1.4% at Room Temperature. *Apl. Mater* 2, 076112. doi:10.1063/1.4891276

Tan, A. J., Huang, M., Avci, C. O., Büttner, F., Mann, M., Hu, W., et al. (2019). Magneto-ionic Control of Magnetism Using a Solid-State Proton Pump. *Nat. Mater* 18, 35–41. doi:10.1038/s41563-018-0211-5

Tkach, A., Kehlberger, A., Büttner, F., Jakob, G., Eisebitt, S., and Kläui, M. (2015). Electric Field Modification of Magnetotransport in Ni Thin Films on (011) PMN-PT Piezosubstrates. *Appl. Phys. Lett.* 106, 062404. doi:10.1063/1.4907775

Wang, C., Pu, J., Hu, Z., Su, W., Guan, M., Peng, B., et al. (2019). Electric Field Tuning of Anisotropic Magnetoresistance in Ni-Co/PMN-PT Multiferroic Heterostructure. *IEEE Trans. Magn.* 55, 1–3. doi:10.1109/tmag.2018.2865250

Wang, J., Huang, Q. K., Lu, S. Y., Tian, Y. F., Chen, Y. X., Bai, L. H., et al. (2018). Reversible Electrical-Field Control of Magnetization and Anomalous Hall Effect in Co/PMN-PT Hybrid Heterostructures. *Appl. Phys. Lett.* 112, 152904. doi:10.1063/1.5022381

Wang, S., Gao, T., Wang, C., and He, J. (2013). Studies of Anisotropic Magnetoresistance and Magnetic Property of Ni81Fe19 Ultra-thin Films with the Lower Base Vacuum. *J. Alloys Compd.* 554, 405–407. doi:10.1016/j.jallcom.2012.12.004

Wang, X., Yang, Q., Wang, L., Zhou, Z., Min, T., Liu, M., et al. (2018). E-Field Control of the RKKY Interaction in FeCoB/Ru/FeCoB/PMN-PT (011) Multiferroic Heterostructures. *Adv. Mat.* 30, 1803612. doi:10.1002/adma.201803612

Wang, Y., Sun, J., Shimada, T., Hirakata, H., Kitamura, T., and Wang, J. (2020). Ferroelectric Control of Magnetic Skyrmions in Multiferroic Heterostructures. *Phys. Rev. B* 102, 014440. doi:10.1103/physrevb.102.014440

Weisheit, M., Fähler, S., Marty, A., Souche, Y., Poinsignon, C., and Givord, D. (2007). Electric Field-Induced Modification of Magnetism in Thin-Film Ferromagnets. *Science* 315, 349–351. doi:10.1126/science.1136629

Xiong, R., Zhang, W., Fang, B., Li, G., Li, Z., Zeng, Z., et al. (2018). Ferromagnetic Resonance Manipulation by Electric Fields in Ni81Fe19/Bi3.15Nd0.85Ti2.99Mn0.01O12 Multiferroic Heterostructures. *Appl. Phys. Lett.* 113, 172407. doi:10.1063/1.5047066

Yamada, S., Teramoto, Y., Matsumi, D., Kepaptsoglou, D., Azaceta, I., Murata, T., et al. (2021). Electric Field Tunable Anisotropic Magnetoresistance Effect in an Epitaxial Co2 Fe Si/Ba TiO3 Interfacial Multiferroic System. *Phys. Rev. Mat.* 5, 014412. doi:10.1103/physrevmaterials.5.014412

Yang, Y., Huang, H., Luo, Z., Gao, C., Li, X., and Tao, C. F. (2017). Electric-field Control of Magnetic Anisotropy Rotation in Multiferroic Ni/(011)-Pb(Mg2/3Nb1/3)0.7Ti0.3O3 Heterostructures. *J. Appl. Phys.* 122, 134105. doi:10.1063/1.4990874

Yang, Y., Luo, Z., Wang, S., Huang, W., Wang, G., Wang, C., et al. (2021). Electric-field-assisted Non-volatile Magnetic Switching in a Magnetoelectronic Hybrid Structure. *iScience* 24, 102734. doi:10.1016/j.isci.2021.102734

Yu, Z.-F., Lu, J., Wang, H.-L., Zhao, X.-P., Wei, D.-H., Ma, J.-L., et al. (2019). Tunable Perpendicular Magnetic Anisotropy in Off-Stoichiometric Full-Heusler Alloy Co2MnAl*. *Chin. Phys. Lett.* 36, 067502. doi:10.1088/0256-307x/36/6/067502

Zhang, S., Zhao, Y. G., Li, P. S., Yang, J. J., Rizwan, S., Zhang, J. X., et al. (2012). Electric-Field Control of Nonvolatile Magnetization inCo40Fe40B20/Pb(Mg1/3Nb2/3)0.7Ti0.3O3Structure at Room Temperature. *Phys. Rev. Lett.* 108, 137203. doi:10.1103/physrevlett.108.137203

Zhang, S., Zhao, Y., Xiao, X., Wu, Y., Rizwan, S., Yang, L., et al. (2015). Giant Electrical Modulation of Magnetization in Co40Fe40B20/Pb(Mg1/3Nb2/3)0.7Ti0.3O3(011) Heterostructure. *Sci. Rep.* 4, 3727. doi:10.1038/srep03727

Zhang, W., Hao, Q., and Xiao, G. (2011). Low-frequency Noise in Serial Arrays of MgO-Based Magnetic Tunnel Junctions. *Phys. Rev. B* 84, 094446. doi:10.1103/physrevb.84.094446

Zhao, C.-J., Ding, L., HuangFu, J.-S., Zhang, J.-Y., and Yu, G.-H. (2013). Research Progress in Anisotropic Magnetoresistance. *Rare Mater.* 32, 213–224. doi:10.1007/s12598-013-0090-5

Zhou, C., Zhu, D., Liu, F., Feng, C., Zhang, M., Ding, L., et al. (2021). Electric-field-induced In-Plane Effective 90° Magnetization Rotation in Co2FeAl/PMN-PT Structure*. *Chin. Phys. B* 30, 057504. doi:10.1088/1674-1056/abd7de

Zhou, W., Ma, C., Gan, Z., Zhang, Z., Wang, X., Tan, W., et al. (2017). Manipulation of Anisotropic Magnetoresistance and Domain Configuration in Co/PMN-PT (011) Multiferroic Heterostructures by Electric Field. *Appl. Phys. Lett.* 111, 052401. doi:10.1063/1.4997322

Conflict of Interest: The authors declare that the research was conducted in the absence of any commercial or financial relationships that could be construed as a potential conflict of interest.

Publisher's Note: All claims expressed in this article are solely those of the authors and do not necessarily represent those of their affiliated organizations, or those of the publisher, the editors and the reviewers. Any product that may be evaluated in this article, or claim that may be made by its manufacturer, is not guaranteed or endorsed by the publisher.

Copyright © 2022 Wang, Huang, Wang, Li, Wei, Sun, Ge, Mao, Li, Yang, Jia, Zhang, Luo and Gao. This is an open-access article distributed under the terms of the Creative Commons Attribution License (CC BY). The use, distribution or reproduction in other forums is permitted, provided the original author(s) and the copyright owner(s) are credited and that the original publication in this journal is cited, in accordance with accepted academic practice. No use, distribution or reproduction is permitted which does not comply with these terms.